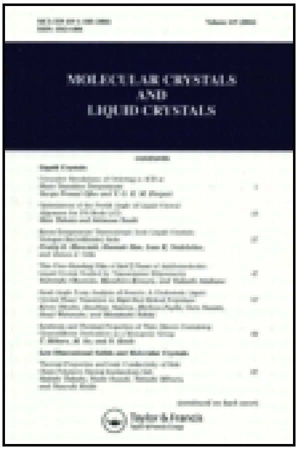

Molecular Crystals and Liquid Crystals
Publication details, including instructions for authors and subscription information:
http://www.tandfonline.com/loi/gmcl20

Nonlinear Dielectric Spectroscopy of MHPOBC

Koji Tanaka [a] , Masatoshi Ichikawa [a] & Yasuyuki Kimura [a]
[a] Department of Physics, School of Sciences, Kyushu University, Higashi-ku, Fukuoka, Japan

Version of record first published: 22 Sep 2010

Mol. Cryst. Liq. Cryst., Vol. 477, pp. 195/[689]–204/[698], 2007

ISSN: 1542-1406 print/1563-5287 online
DOI: 10.1080/15421400701684020

Nonlinear Dielectric Spectroscopy of MHPOBC

Koji Tanaka
Masatoshi Ichikawa
Yasuyuki Kimura
Department of Physics, School of Sciences, Kyushu University,
Higashi-ku, Fukuoka, Japan

We apply nonlinear dielectric spectroscopy to an antiferroelectric liquid crystal MHPOBC at various smectic sub-phases. In the SmC_α^* phase, the third-order nonlinear dielectric spectrum ε_3^* is found to be composed of the contributions from ferroelectric soft mode and soft mode of the SmC_α^* phase. The obtained spectrum is well ascribable by the theoretical one calculated by the Landau-type of phenomenological theory. In the SmC^* phase, ε_3^* shows a complicated form, and is different from one observed in usual ferroelectric liquid crystals. In the SmC_{FI1}^*(SmC_γ^*) phase, ferrielectric Goldstone mode with broad distribution of relaxation times is observed in both ε_1^* and ε_3^*.

Keywords: antiferroelectric liquid crystal; MHPOBC; nonlinear dielectric spectroscopy; SmC^*; SmC_α^*; SmC_{FI1}^*

1. INTRODUCTION

Antiferroelectric liquid crystals (AFLCs) have been intensively studied experimentally and theoretically since its discovery because of their potential for display application and their interesting physical properties [1]. These materials usually show various kinds of smectic phases. For example, MHPOBC (4-(1-methylheptyl oxycarbonyl) phenyl 4'-octyloxy-biphenyl-4-carboxylate) shows SmA, SmC_α^*, SmC^*, SmC_{FI1}^* (SmC_γ^*) and SmC_A^* phases on cooling [2].

This work is supported by Grant-in-Aid for Scientific Research from the Ministry of Education, Culture, Sports, Science and Technology of Japan.

Address correspondence to Yasuyuki Kimura, Department of Physics, Graduate School of Sciences, Kyushu University, 6-10-1 Hakozaki, Higashi-ku, Fukuoka 812-8481, Japan. E-mail: kim8scp@mbox.nc.kyushu-u.ac.jp

Linear dielectric measurement is one of the useful methods to study the phase sequence and the polar structure of antiferroelectric liquid crystals [3]. However, it is difficult to detect the antiferroelectric modes in the antiferroelectric (SmC_A^*) phase by linear dielectric response. It is due to the local cancellation of the spontaneous polarization by its antiferroelectric ordering of molecules [4]. But, since there exists nonlinear coupling between dielectric anisotropy and electric field, the relaxation modes those are hard to detect by linear dielectric measurement can be observed by nonlinear dielectric spectroscopy [5].

In the SmC_α^* phase, the tilt order parameter ξ_q at the SmA-SmC_α^* phase transition does not linearly couple with electric field. We cannot obtain the detail information on its dynamics by linear dielectric measurement. But, ξ_q couples square of electric field, and we can obtain the information on its dynamics by nonlinear dielectric measurement [6,7].

The SmC^* phase is ferroelectric phase and the main relaxation mode in this phase is ferroelectric Goldstone mode. Since the spontaneous polarization couples electric field linearly in this phase, the Goldstone mode is possible to detect by both the linear and nonlinear dielectric responses. We can obtain various physical quantities in the SmC^* phase easily from the parameters of linear and nonlinear dielectric spectrum [8].

The SmC_{FI1}^*(SmC_γ^*) is ferrielectric phase and its unit-cell is 3-layers [9,10]. The ferrielectric Goldstone mode can be detected by the linear response because spontaneous polarization is not completely cancelled. Although it has been reported that SmC_γ^* phase shows helical structure with a long pitch and has many orientational defects [11], the details of its dynamics have not been understood well. It is expected to obtain more detailed information on the dynamics of the SmC_{FI1}^* by nonlinear dielectric response.

In this study, we apply the nonlinear dielectric measurement to the smectic sub-phases of a typical antiferroelectric liquid crystal, MHPOBC. We also discuss its response theoretically by using the phenomenological equation of motion and compare them with the experimental ones.

2. EXPERIMENT

Under a weak electric field E, the electric displacement D can be expanded into the power series of E as $D = \sum_{m=1}^{\infty} \varepsilon_m E^m$. When the applied field is a sinusoidal one, $E = E_0 \cos \omega t$ (E_0: amplitude, ω: angular frequency), D is written as a sum of the fundamental D_1^* and the higher harmonic components D_m^* ($m = 2,3,\ldots.$) of ω[12]. In our case, the even-order harmonic components disappear due to the symmetry of polarization to electric field. When the applied field E_0 is small, the dominant term in D_m^* is proportional to E_0^m. We can experimentally obtain the mth-order nonlinear dielectric spectrum ε_m^* from the applied field E_0 dependence of D_m^* as

$$\varepsilon_m^* = \lim_{E_0 \to 0} \frac{D_m^*}{E_0^m} \cdot 2^{m-1} \equiv \varepsilon_m' - i\varepsilon_m''. \qquad (1)$$

The sinusoidal electric field generated from a synthesizer (HP33120A) in the frequency range from 1 Hz to 1 MHz was applied to a sample after passing through a low-pass filter (NF3628) to reduce the harmonic distortion in $E(t)$. The electric displacement D detected by a charge amplifier was digitized, averaged and transformed into complex spectrum data on a vector signal analyzer (HP89410A). The cell was mounted on a hot stage and its temperature was controlled with an accuracy of 0.05 K by a temperature controller (LS340).

The surfaces of the cells are spin-coated with polyimide and rubbed unidirectionally to attain homogeneous alignment of liquid crystals. The thickness of a sample is about 19 μm and the area of ITO electrode is 16 mm^2.

3. RESULTS AND DISCUSSIONS

3.1. Electric Field *E* Dependence of Electric Displacement D_m^*

Figure 1 shows the dependence of the imaginary part of complex electric displacement D_m^* on E_0^m obtained in the SmC$_\alpha^*$ phase. D_1^* and D_3^*

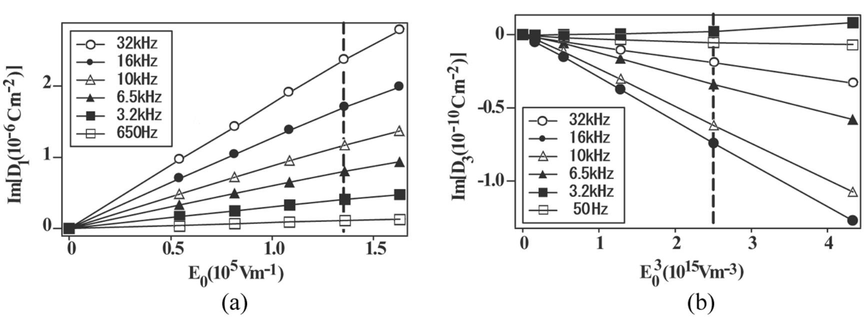

FIGURE 1 Applied electric field E_0 dependence of the imaginary part of D_1^* and D_3^* in the SmC$_\alpha^*$ phase.

are the fundamental and the third-order harmonic components of D^*, respectively. Within the range of the electric field we applied, the electric displacement D_m^* shows the linear relations with E_0^m. The broken line in Figure 1 indicates the amplitude of the electric field we apply in the measurement of temperature dependence of ε_1^* and ε_3^*.

3.2. Temperature Dependence of Linear and Third-Order Nonlinear Permittivity

Figure 2 shows the temperature dependence of the real part of the linear ε_1' and third-order nonlinear dielectric permittivity ε_3' at 32 Hz. Both ε_1' and ε_3' increase near the SmA- SmC$_\alpha^*$ phase transition. This increase is attributed to the contribution of soft mode. In the SmC* phase of typical ferroelectric liquid crystals, the sign of ε_3' at low frequency is negative. But in the SmC* phase of MHPOBC, the change of its sign is observed. The magnitude of linear permittivity

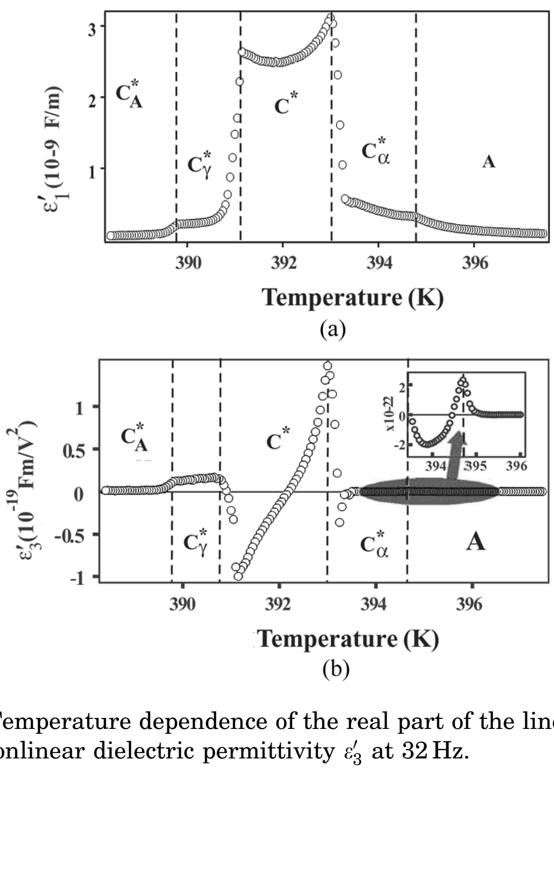

FIGURE 2 Temperature dependence of the real part of the linear ε_1' and the third-order nonlinear dielectric permittivity ε_3' at 32 Hz.

ε_1^* gives information on respective phases, but the magnitude and sign of ε_3^* gives more detailed information on sub-phases.

3.3. Nonlinear Dielectric Response in the SmC$_\alpha^*$ Phase

In the SmC$_\alpha^*$ phase, c-director forms helical structure and its pitch is about several layers [10]. We discuss the dielectric response in the SmC$_\alpha^*$ phase near $T_{A\text{-}C\alpha^*}$ phase transition by the phenomenological free-energy of Landau-type. The experimentally obtained spectra are shown in Figure 3. Although the obtained spectrum of ε_1^* is a single relaxation of Debye-type [7,13], ε_3^* shows complex frequency spectrum. In order to discuss the complex profile of ε_3^*, we calculate ε_3^* by using the phenomenological theory of Landau type [6].

Landau free-energy density f near the SmA-SmC$_\alpha^*$ phase transition can be written with the ferroelectric tilt order parameter ξ_f and that of SmC$_\alpha^*$ phase ξ_q [7] as,

$$f = \frac{1}{2}\alpha_f\xi_f^2 + \frac{1}{4}\alpha_f\xi_f^4 + \frac{1}{2}\alpha_q\xi_q^2 + \frac{1}{4}\alpha_q\xi_q^4 + \frac{1}{2}\eta\xi_f^2\xi_q^2 + \lambda_f\chi_f\xi_f E - \frac{1}{4}\varepsilon_a\xi_q^2 E^2, \quad (2)$$

where η is the coupling constant between two order parameters, χ_f is the permittivity without coupling between the polarization and the order parameter, λ_f is the piezoelectric constant and ε_a is the dielectric anisotropy. From the Landau-Khalatnikov equation, the theoretically

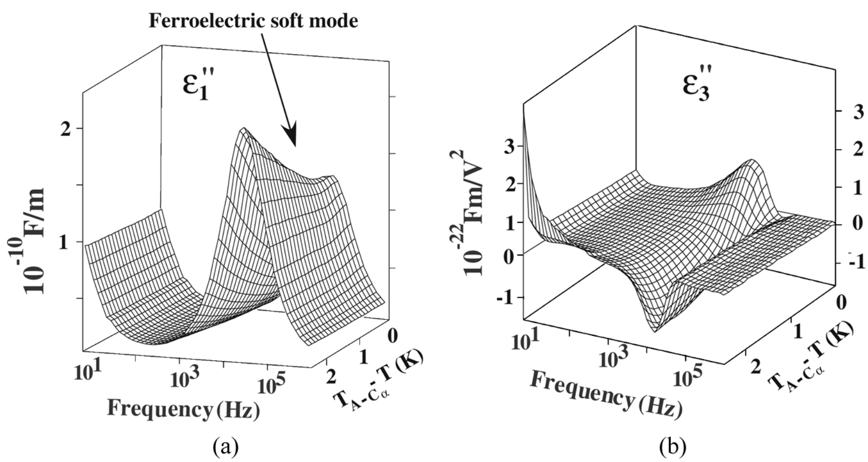

FIGURE 3 The imaginary part of the linear ε_1'' and the third-order nonlinear dielectric spectrum ε_3'' as a function of temperature in the SmC$_\alpha^*$ phase.

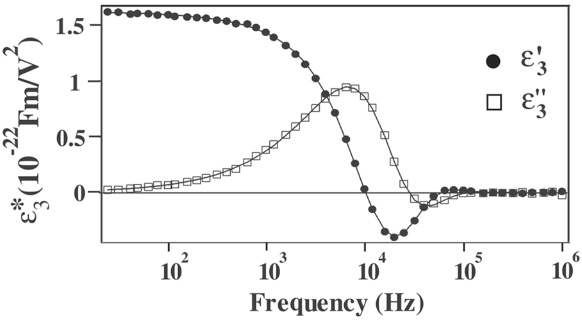

FIGURE 4 Typical spectrum of ε_3^* in the SmC$_\alpha^*$ phase at $T_{\text{A-C}\alpha}$-$T = 0.05\,\text{K}$. The solid lines represent the best-fitted curves of Eq. (3) to data (filled and empty circles).

calculated third-order nonlinear permittivity ε_3^* is given as

$$\varepsilon_3^* = \frac{-\beta_f(\lambda_f\chi_f)^4/v^4}{(1+i\omega\tau_f)^3(1+3i\omega\tau_f)} + \frac{\xi_{qo}^2/2u}{1+2i\omega\tau_q}\left[\varepsilon_a - \frac{2\eta\chi_f^2\lambda_f^2/v^2}{(1+i\omega\tau_f)^2}\right]\left[\varepsilon_a - \frac{6\eta\chi_f^2\lambda_f^2/v^2}{(1+i\omega\tau_f)(1+3i\omega\tau_f)}\right], \quad (3)$$

where $u = \alpha_q + 3\beta_q\xi_{q0}^2$, $v = \alpha_f + \eta\xi_{q_0}^2$, $\tau_q = \gamma/u$, $\tau_f = \gamma/v$, ξ_{q0} is the order parameter without field and γ is the viscosity. We fitted the spectrum of ε_3^* to Eq. (3) taking into account the distribution of relaxation times. Figure 4 shows the typical spectrum of ε_3^* in the SmC$_\alpha^*$ phase, and the solid lines are the best-fitted spectrum of Eq. (3).

From the result of fitting, the contribution of dielectric anisotropy term in Eq. (3) is found to be several times smaller than that of the coupling term near the SmA- SmC$_\alpha^*$ phase transition temperature $T_{\text{A-C}\alpha}$. The increment of soft mode of the SmC$_\alpha^*$ phase shows a clear peak, and the relaxation frequency f_q ($\equiv 1/2\pi\tau_q$) takes minimum value just below $T_{\text{A-C}\alpha}$. We find that the temperature dependence of f_q shows Curie-Weiss type critical behavior near the SmA-SmC$_\alpha^*$ phase transition. Therefore the critical behavior of ε_3^* is confirmed to be due to that of soft mode ξ_q.

3.4. Nonlinear Dielectric Response in the SmC* Phase

We discuss the dielectric spectrum in the SmC* phase. We can detect the ferroelectric Goldstone mode in both ε_1^* and ε_3^*. The spatial distribution of the azimuthal angle ϕ along the helical axis under an ac electric field, $E = E\cos\omega t$, satisfies the following torque balance equation [8,12];

$$K\frac{\partial^2\phi}{\partial z^2} - \gamma\frac{\partial\phi}{\partial t} = P_s E\sin\phi\,, \tag{4}$$

where K is the effective elastic constant and γ is the rotational viscosity. The third-order nonlinear dielectric spectrum ε_3^* is calculated as follows,

$$\varepsilon_3^* = \frac{\Delta\varepsilon_3\{1+(i\omega\tau_3)^2/3+5(i\omega\tau_3)/3\}}{\{1+(i\omega\tau_3)\}^3\{1+3(i\omega\tau_3)\}\{1+(i\omega\tau_3)/2\}}, \tag{5}$$

where $\tau_3 = \gamma/Kq_0^2$, and q_0 is the wave number of helix.

The obtained spectrum of ε_3^* shows a complicated form which is different from one observed in typical ferroelectric liquid crystals. The different behavior seems to relate to the existence of neighboring sub-phases (SmC_α^*, SmC_γ^*). Optical purity has great influence on the phase sequence [3,14]. In the case of MHPOBC, when optical purity reduces, the phase sequence changes to SmA-SmC*-$\mathrm{SmC}_\mathrm{A}^*$. To study the dependence of ε_3^* on optical purity, we also measured ε_3^* for the samples whose optical purity are 60%and 40%. We call them sample-A (60%), and sample-B (40%), respectively. The experimentally obtained spectra of ε_3' are shown in Figure 5.

The temperature range of SmC* phase in respective samples are about 2 K (pure sample), about 7 K (sample-B, sample-C). In racemized samples, we can fit the spectrums of ε_3^* to Eq. (5) at the higher temperature region of SmC* phase. We obtained the spectrums of ε_3^* with broad distribution of relaxation time at the lower temperature in racemized samples. From the result of linear dielectric spectrum, we find that the pitch of helix increases with the optical purity decreases. Therefore the reason why we cannot fit the spectrum of ε_3^* at the lower temperature by Eq. (5) is that the spectrum of ε_3^* shows long-pitched distorted structure at the lower temperature in racemized samples.

On the other hand, the spectrum ε_3^* in pure sample shows a complicated form, and we cannot fit it to Eq. (5). In this case, the temperature range of SmC* phase is very narrow compared with racemized samples. Moreover, SmC_α^*-SmC* and SmC*-$\mathrm{SmC}_\mathrm{FI1}^*$ phase transitions are first order. Therefore, in the SmC* phase of pure sample, there is the possibility that SmC_α^* and SmC* phases or SmC* and $\mathrm{SmC}_\mathrm{FI1}^*$ phases coexist. We consider that the spectrum ε_3^* of pure sample suffers serious influence of sub-phases (SmC_α^*, $\mathrm{SmC}_\mathrm{FI1}^*$).

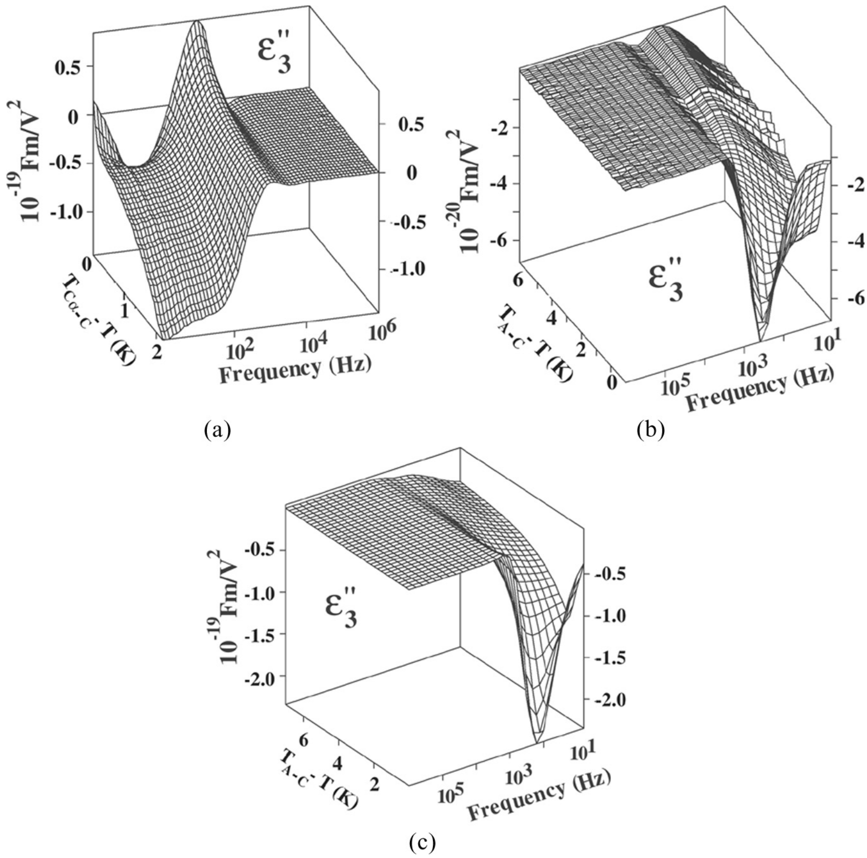

FIGURE 5 The imaginary part of the third-order nonlinear dielectric permittivity ε_3'' as a function of temperature. (a) pure MHPOBC, (b) sample-A (60% in optical purity), (c) sample-B (40% in optical purity).

3.5. Nonlinear Dielectric Response in the SmC$^*_{FI1}$ (SmC$^*_\gamma$) Phase

The experimentally obtained spectra of ε_1'' and ε_3'' are shown in Figure 6. ε_1^* and ε_3^* exhibit a spectrum with broad distribution of relaxation times. In the spectrum of ε_1^*, the relaxation mode which exists at the low frequency is due to the ferrielctric Goldstone mode. In the spectrum of ε_3^*, the relaxation mode with positive increment is observed at about 120 Hz. We consider that this relaxation mode corresponds to ferrielectric Goldstone mode.

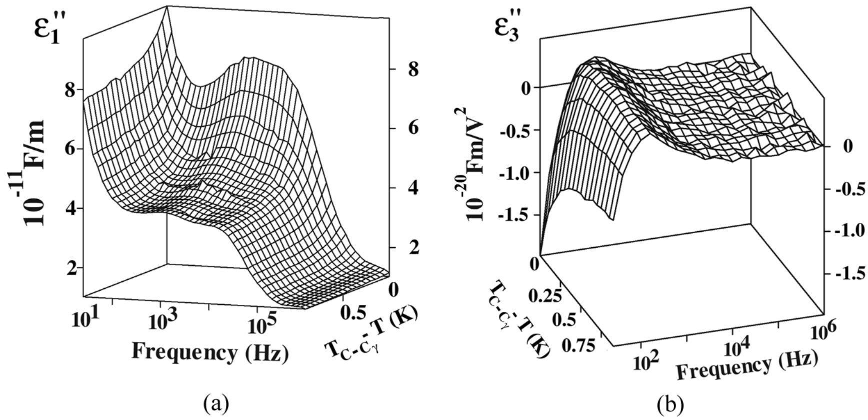

FIGURE 6 The imaginary part of the linear ε_1'' and third-order nonlinear dielectric permittivity ε_3'' as a function of temperature.

4. CONCLUSION

We have applied the nonlinear dielectric spectroscopy to the various smectic sub-phases in an antiferroelectric liquid crystal MHPOBC. Nonlinear dielectric spectroscopy enables us to obtain detail information which cannot be obtained by linear one. We detected the spectrum of ε_3^* corresponding to the soft mode of SmC_α^* phase near SmA-SmC_α^* phase transition. We discussed it by the phenomenological free energy of Landau-type. We find that the critical behavior of ε_3^* is due to that of soft mode ξ_q. In the case of the SmC^* phase, we measured three samples with different optical purity. From the relaxation spectrum of ε_1^*, we find that the pitch of helix increases with the decrease of optical purity. The higher temperature region of SmC^* phase of MHPOBC (100% in optical purity) is considered to be affected by coexistence of neighboring phases. In the case of SmC_γ^* phase, we detected the ferrielectric Goldstone mode in both spectrum of ε_1^* and ε_3^*.

REFERENCES

[1] Fukuda, A., Takanishi, Y., Isozaki, T., Ishikawa, K., & Takezoe, H. (1994). *J. Mater. Chem.*, *4*, 997.
[2] Gorecka, E., Chandani, A. D. L., Ouchi, Y., Takezoe, H., & Fukuda, A. (1990). *Jpn. J. Appl. Phys.*, *29*, 131.
[3] Takezoe, H., Hiraoka, K., Isozaki, T., Miyachi, K., Aoki, H., & Fukuda, A. (1993). Dielectric properties in antiferroelectric liquid crystals. In: *Modern Topics in Liquid Crystals*, Buka, A. (Ed.), World Scientific: Singapore, p. 319.

[4] Chandani, A. D. L., Gorecka, E., Ouchi, Y., Takezoe, H., & Fukuda, A. (1989). *Jpn. J. Appl. Phys.*, *28*, L1265.
[5] Kimura, Y., Hayakawa, R., Okabe, N., & Suzuki, Y. (1996). *Phys. Rev. E*, *53*, 6080.
[6] Kimura, Y., Isono, H., & Hayakawa, R. (2002). *Eur. Phys. J. E*, *9*, 3.
[7] Bourny, V. & Orihara, H. (2001). *Phys. Rev. E*, *63*, 021703.
[8] Kimura, Y., Hara, S., & Hayakawa, (2000). *R. Phys. Rev. E*, *62*, R5907.
[9] Johnson, P. M., Olson, D. A., Pankratz, S., Nguyen, T., Goodby, J., Hird, M., & Huang, C. C. (2000). *Phys. Rev. Lett.*, *84*, 4870.
[10] Mach, P., Pindak, R., Levelut, A.-M., Barois, P., Nguyen, H. T., Huang, C. C., & Furenlid, L. (1998). *Phys. Rev. Lett.*, *81*, 1015.
[11] Muševič, I., Škarabot, M., Heppke, G., & Nguyen, H. T. (2002). *Liq. Cryst.*, *29*, 1565.
[12] Kimura, Y. & Hayakawa, R. (1993). *Jpn. J. Appl. Phys.*, *32*, 4571.
[13] Hiraoka, K., Taguchi, A., Ouchi, Y., Takezoe, H., & Fukuda, A. (1990). *Jpn. J. Appl. Phys.*, *29*, L103.
[14] Vaupotič, N. & Čepič, M. (2005). *Phys. Rev. E*, *71*, 041701.